ADITUM
Enrich your Research

International Journal of Epidemiology and Public Health Research

Research Article

Theoretical investigation on Tf_2O-catalyzed [3 + 2 + 1] benzannulation of enaminone and ac-ylacetonitrile leading to multisubstituted arylnitrile

Nan Lu*, Junling Duan
College of Chemistry and Material Science, Shandong Agricultural University, Taian 271018, P. R. China.

Article Info

Received: April 01, 2025
Accepted: April 10, 2025
Published: April 15, 2025

***Corresponding author:** Nan Lu, College of Chemistry and Material Science, Shandong Agricultural University, Taian 271018, P. R. China.

Citation: Nan Lu, Junling Duan. (2025) "College of Chemistry and Material Science, Shandong Agricultural University, Taian 271018, P. R. China". International Journal of Epidemiology and Public Health Research, 6(2); DOI: 10.61148/2836-2810/IJEPHR/122.

Abstract

The first theoretical investigation was provided by our DFT calculation on Tf_2O-catalyzed [3 + 2 + 1] benzannulation of annular-enaminone with monomeric benzoyl acetonitrile. Initially activated by Tf_2O, enaminone was formed vinyl iminium triflate intermediate, which was captured by benzoyl acetonitrile to initiate selective 1,2-addition and form first TfOH. Subsequently, key trifluorome-thanesulfonate intermediate was generated after elimination of dimethylamine. Next with a second molecule of benzoyl acetonitrile, the reaction took place via Michael-type addition followed by second proton donation. Then competitive 1,4-elimination or 1,2-elimination were possible to complete the release of second TfOH. Finally, the product multisubstituted arylnitrile was obtained through sequential Knoevenagel condensation and aromatization. Michael-type addition was determinate to be rate-limiting from the perspective of whole process. The 1,2-elimination was more favorable within two parallel paths from kinetics.

Keywords: arylnitrile; Tf_2O; [3+2+1] benzannulation; Knoevenagel condensation; trifluorome-thanesulfonate

Introduction

As common functional group, CN is easily converted into aldehydes and amidines. This makes aromatic nitriles versatile organic synthons for a wide range of natural products and agricultural chemicals [1,2]. Many cross-coupling reactions were efficient to synthesize aromatic nitriles [3-5]. In recent years, many efforts have been focused on benzannulation offering a powerful strategy for constructing aromatic rings from acyclic precursors. Du reported Copper-catalyzed [3 + 2 + 1] cycloaddition of alkenes with benzoquinones and dicarbonyl compounds [6]. Chen explored [3 + 3] cycloaddition reaction of vinyl sulfoxonnium ylides with cyclopropenones [7]. Wei researched [2 + 2 + 1 + 1] cycloaddition for de novo synthesis of densely functionalized phenols [8]. There are also base-mediated benzannulation of α-cyanocrotonates with ynones and five-component [2 + 2 + 1 + 1] tandem benzannulation to multifunctionalized aromatic amines [9,10].

A versatile class of push−pull olefin we are interested in is enaminone as promising precursor for various aromaticcompounds [11,12]. For instance, Zeng discovered photocatalytic pyridine synthesis with enaminones and TMEDA under metal-free conditions [13]. Fan researched Co(III)-catalyzed coupling of enaminones with oxadiazolones for imidazole synthesis [14]. Zhang reported Silver-catalyzed cascade bis-heteroannulation reaction of enynones and o-hydroxyphenyl enaminones to access highly functionalized 3-furylmethyl chromones [15]. Duan gave chemodivergent synthesis of polysubstituted pyrroles and pyridines via tandem site-selective bromination and highly regioselective Heck reaction of N-allyl enaminones [16]. Usually, enaminone participates in benzannulation as Cn synthon. Such as redox neutral [4 + 2] benzannulation of dienals and tertiary enaminones in

benzaldehyde synthesis, Copper (II)-catalyzed [2 + 2+2] annulation of enaminones with maleimides using traceless directing group, [3 + 3] condensation reaction from tricarbonyl compounds and enaminones, cinnamaldehydes for synthesis of polysubstituted phenols, and [5 + 1] cyclizations via cleavage of 1,3-dicarbonyls to synthesize highly functionalized naphthols [17-20]. However, [3+ 2 + 1] benzannulation remained less.

In this field, trifluoromethanesulfonic anhydride (Tf_2O) is an efficient activation reagent for carbonyl derivatives [21]. Zhang group has made many contributions in converting enaminones into vinyl iminium triflates. The previous work includes one-pot synthesis of 3-amino diynes via Cu(I)-catalyzed reaction with terminal alkynes, Tf_2O-mediated tandem reaction to functionalized conjugated-enals/β-naphthalaldehydes, and divergent synthesis of enynals and dihydrobenzo[f]isoquinolines [22-24]. Another breakthrough was Tf_2O-mediated [3 + 2 + 1] benzannulation of enaminones with acylacetonitriles [25]. Although multisubstituted arylnitriles were synthesized, many problems in experiment still puzzled requiring an in-depth theoretical study for this strategy. How annular-enaminone was activated by Tf_2O to form vinyl iminium triflate? How crucial trifluorome-thanesulfonate intermediate was generated during elimination of dimethylamine? What's the detailed process of sequential Knoevenagel condensation and aromatization following either 1,4- or 1,2-elimination?

2 Computational details

Structures were optimized at M06-2X/6-31G(d) level with GAUSSIAN09 [26]. Among various DFT methods [27], M06-2X functional has smaller deviation between experimental and calculated value than B3LYP hybrid functional [28,29]. With 6-31G(d) basis set, it can provide best compromise between time consumption and energy accuracy. It was also found to give accurate results for stepwise (2 + 2) cycloaddition, enantioselective (4 + 3) and Diels−Alder reaction [30,31]. Together with good performance on noncovalent interaction, it is suitable for this system [32-34]. To obtain zero-point vibrational energy (ZPVE), harmonic frequency calculations were carried out at M06-2X/6-31G(d) level gaining thermodynamic corrections at 353 K and 1 atm in dichloromethane (DCM). At M06-2X/6-311++G(d,p) level, the solvation-corrected free energies were obtained using integral equation formalism polarizable continuum model (IEFPCM) [35-39] on M06-2X/6-31G(d)-optimized geometries. NBO procedure was performed with Natural bond orbital (NBO3.1) obtaining lone pair and bond to characterize bonding orbital interaction and electronic properties [40-42]. Using Multiwfn_3.7_dev package [43].

3 Results and Discussion

The mechanism was explored for Tf_2O-catalyzed [3 + 2 + 1] benzannulation of annular-enaminone **1** with monomeric benzoylacetonitrile **2** to multisubstituted arylnitrile **3** (Scheme 1). Illustrated by black arrow of Scheme 2, under the activation of Tf_2O, enaminone **1** formed vinyl iminium triflate intermediate **A**, which was subsequently captured by benzoyl acetonitrile **2** to initiate selective 1,2-addition forming intermediate **B** and TfOH. Subsequently, key trifluorome-thanesulfonate intermediate **4** was generated after elimination of dimethylamine from **B**. Then Michael-type addition of **4** reacted with a second molecule of **2** gave intermediate **C** followed by second proton donation from **2**. The intermediates **D** or **E** were yielded via competitive 1,4-elimination (red arrow) or 1,2-elimination (blue arrow) after the release of a second TfOH. Finally, sequential Knoevenagel condensation and aromatization occurred resulting in final product multisubstituted arylnitrile (**D** to **F** to **3**, or **E** to **G** to **3**). Figure 1 listed schematic structures of optimized TSs in Scheme 2. Table 1 gave activation energy for all steps.

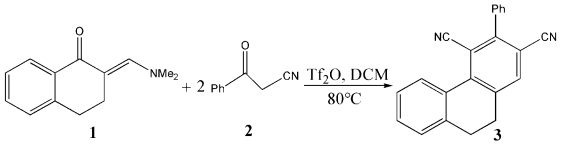

Scheme 1 Tf_2O-catalyzed [3 + 2 + 1] benzannulation of annular-enaminone **1** with monomeric benzoylacetonitrile **2** to access multisubstituted arylnitrile **3**.

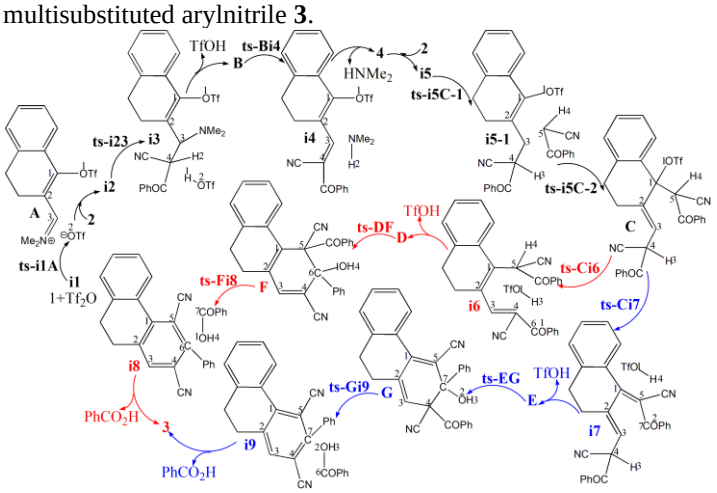

Scheme 2 Reaction mechanism of Tf_2O-catalyzed [3 + 2 + 1] benzannulation of **1** with **2** to access **3**.

3.1 Vinyl iminium triflate formation/selective 1,2-addition/dimethylamine elimination

Initially from complex **i1** binding enaminone **1** and catslyst Tf_2O, vinyl iminium triflate intermediate **A** was formed via **ts-i1A** in step 1 with low activation energy of 2.9 kcal mol^{-1} exothermic by -25.0 kcal mol^{-1} (black dash line of Figure 1a). The transition vector includes one Tf leaving from Tf_2O bonding to carbonyl of **1** that is O2···S···O1 (1.84, 2.17 Å). The activation of Tf_2O is revealed through small barrier and the resultant **A** rather stable.

Subsequently, the intermediate **i2** was taken as new starting point afte **A** captured by benzoyl acetonitrile **2**. Thus selective 1,2-addition was initiated via **ts-i23** in step 2 with activation energy of 17.5 kcal mol^{-1} exothermic by -11.4 kcal mol^{-1} generating **i3**. Prior to the nucleophilic addition of C4 of **2** to C3 of **1**, the transition vector also demonstrates concerted proton transfer C4···H1···O2 (2.39, 1.81, 1.23 Å). Once C3-C4 typical single bond was formed, the first molucule of TfO2H1 was also obtained. After the removal of TfOH, stable intermediate **B** was in hand for next step.

Via **ts-Bi4**, dimethylamine elimination occurs in step 3 with activation energy of 27.3 kcal mol^{-1} exothermic by -6.6 kcal mol^{-1} delivering intermediate **i4**. The transition vector corresponds to dissociation of NMe_2 from C3, H2 from C4 and the resulting linkage of H···NMe_2 as $HNMe_2$ molecule, strengthened C3=C4 new double bond (1.67, 1.46, 1.31, 1.55 Å) (Figure S1a). When dimethylamine $HNMe_2$ was eliminated, the key trifluorome-thanesulfonate intermediate was generated denoted as **4** involving stable conjugated diene structure.

Table 1 The activation energy (in kcal mol^{-1}) of all reactions in gas and solvent

TS	$\Delta G^{\neq}_{gas}$	$\Delta G^{\neq}_{sol}$
ts-i1A	4.6	2.9
ts-i23	22.6	17.5
ts-Bi4	30.2	27.3
ts-i5C-1	35.1	29.3
ts-i5C-2	32.6	27.6
ts-Ci6	19.9	17.4
ts-Ci7	19.4	16.6
ts-DF	38.0	31.9
ts-Fi8	29.9	20.1
ts-EG	29.8	27.3
ts-Gi9	19.6	14.8

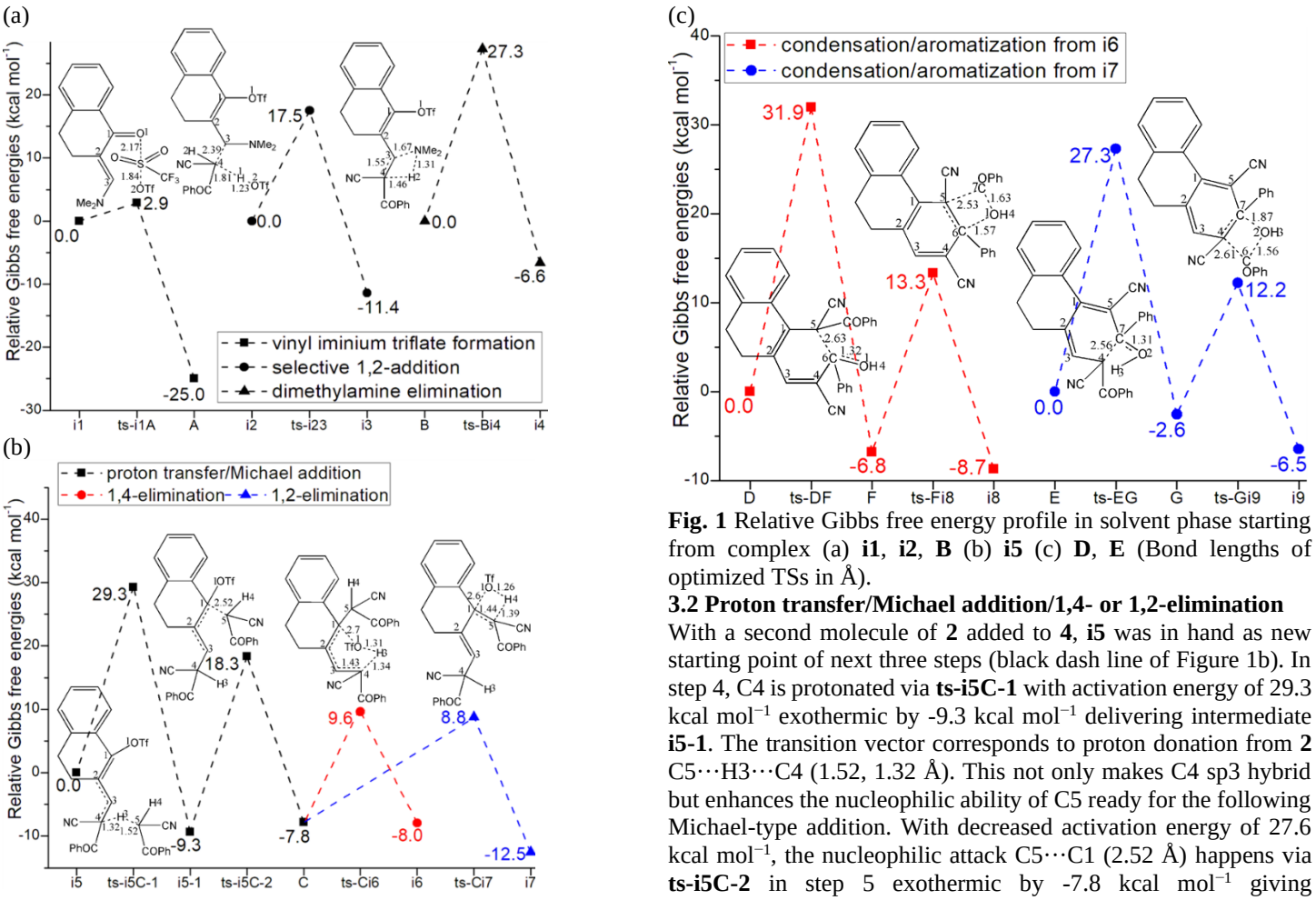

Fig. 1 Relative Gibbs free energy profile in solvent phase starting from complex (a) **i1**, **i2**, **B** (b) **i5** (c) **D**, **E** (Bond lengths of optimized TSs in Å).

3.2 Proton transfer/Michael addition/1,4- or 1,2-elimination

With a second molecule of **2** added to **4**, **i5** was in hand as new starting point of next three steps (black dash line of Figure 1b). In step 4, C4 is protonated via **ts-i5C-1** with activation energy of 29.3 kcal mol^{-1} exothermic by -9.3 kcal mol^{-1} delivering intermediate **i5-1**. The transition vector corresponds to proton donation from **2** C5···H3···C4 (1.52, 1.32 Å). This not only makes C4 sp3 hybrid but enhances the nucleophilic ability of C5 ready for the following Michael-type addition. With decreased activation energy of 27.6 kcal mol^{-1}, the nucleophilic attack C5···C1 (2.52 Å) happens via **ts-i5C-2** in step 5 exothermic by -7.8 kcal mol^{-1} giving

intermediate **C**. The double bond turns to be located on C2=C3 in **C**.

Then competitive 1,4- or 1,2-elimination (red, blue dash line of Figure 1b) were possible for step 6. The common point is cleavage of TfO1 from C1 via C1⋯O1 breaking. The difference lies in through **ts-Ci6**, H3 is departed from C4 to O1 as TfO1H3 while H4 is disruptured from C5 to O1 as TfO1H4 via **ts-Ci7**. The activation energy is 17.4, 16.6 kcal mol^{-1} exothermic by -8.0, -12.5 kcal mol^{-1} generating **i6**, **i7** respectively. The transition vector is also similar with the case of **ts-Ci7** including C1⋯O1 and C5⋯H4⋯O1 (2.6, 1.39, 1.26 Å) (Figure S1b). After the release of a second TfOH molecule from **i6** or **i7**, the intermediates **D** or **E** were yielded with recovered conjugated diene structure of **4** yet different position.

3.3 Parallel Knoevenagel condensation and aromatization

The sequential Knoevenagel condensation and aromatization occurred from **D** or **E** in parallel mode both leading to final product multisubstituted arylnitrile **3**. Via **ts-DF** in step 7, the activation energy of 31.9 kcal mol^{-1} exothermic by -6.8 kcal mol^{-1} affording ring closure of **F** (red dash line of Figure 1c). The transition vector includes closure of six membered ring via C5⋯C6 bonding and cooperative stretching of C6⋯O1 from double to single (2.63, 1.32 Å). Besides novel hydroxyl O1H4, typical C5-C6 single bond is available in **F**, from which the aromatization proceeds via **ts-Fi8** in step 8 with activation energy is 20.1 kcal mol^{-1} exothermic by -8.7 kcal mol^{-1} generating **i8**. The transition vector contains breaking of C5⋯C7, C6⋯O1 as well as C7⋯O1 connecting as PhCOOH molecule and contracted C5-C6 from single to double completing aromatization.

Alternatively via **ts-EG** in step 7, the activation energy is reduced to be 27.3 kcal mol^{-1} exothermic by -2.6 kcal mol^{-1} realizing **G** (blue dash line of Figure 1c). The transition vector indicates nucleophilic approach of C4⋯C7 (2.24 Å) and C7⋯O2 stretching from double to single (2.56, 1.31 Å) (Figure S1c). The structure of **G** is characterized by hydroxyl O2H3 and C4-C7 single bond ready for aromatization via **ts-Gi9** in step 8 with activation energy of 14.8 kcal mol^{-1} exothermic by -6.5 kcal mol^{-1} generating **i9**. The transition vector includes PhCO, O2H3 breaking via C4⋯C6, C7⋯O2 and PhCOOH molecule formation via C6⋯O2 connecting, aromatization via C4=C7 contraction from single to double (2.61, 1.87, 1.56 Å) (Figure S1d). From the perspective of whole process, Michael-type addition was determinated to be rate-limiting step. The 1,2-elimination was more favorable within two parallel paths kinetically.

Table S1. Calculated relative energies (all in kcal mol^{-1}, relative to isolated species) for the ZPE-corrected Gibbs free energies (ΔG_{gas}), Gibbs free energies for all species in solution phase (ΔG_{sol}) at 353 K by M06-2X/6-311++G(d,p)//M06-2X/6-31G(d) method and difference between absolute energy.

Species	ΔG_{gas}	$\Delta G_{sol(EtOH)}$
1+Tf2O	0.00	0.00
i1	-11.14	-6.51
ts-i1A	-6.59	-3.66
A	-19.85	-31.50
A+2	0.00	0.00
i2	-2.50	-3.85
ts-i23	20.13	13.64
i3	-12.63	-15.26
i3-TfOH	0.00	0.00
B	26.89	26.43
ts-Bi4	57.08	53.68
i4	20.73	19.81
i4-HNMe2	0.00	0.00
4	-3.58	-4.86
4+2	0.00	0.00
i5	-4.85	-8.58
ts-i5C-1	30.21	20.71
i5-1	-15.72	-17.92
ts-i5C-2	16.87	9.76
C	-10.43	-16.37
ts-Ci6	9.46	1.01
i6	-10.49	-16.54
ts-Ci7	9.02	0.20
i7	-13.99	-21.11
i6-TfOH	0.00	0.00
D	2.63	-0.87
ts-DF	40.62	31.07
F	-6.03	-7.71
ts-Fi8	23.86	12.41
i8	-6.84	-9.60

i8-PhCOOH	0.00	0.00
3	-29.13	-25.67
i7-TfOH	0.00	0.00
E	-5.27	-8.08
ts-EG	24.56	19.23
G	-6.15	-10.67
ts-Gi9	13.41	4.14
i9	-10.78	-14.56

Table S2. The activation energy (local barrier) (in kcal mol^{-1}) of all reactions in the gas, solution phase calculated with M06-2X/6-311++G(d,p)//M06-2X/6-31G(d) method.

TS	$\Delta G^{\neq}_{gas}$	$\Delta G^{\neq}_{sol}$
ts-i1A (134i)	4.6	2.9
ts-i23 (112i)	22.6	17.5
ts-Bi4 (1596i)	30.2	27.3
ts-i5C-1 (1091i)	35.1	29.3
ts-i5C-2 (346i)	32.6	27.6
ts-Ci6 (1182i)	19.9	17.4
ts-Ci7 (996i)	19.4	16.6
ts-DF (287i)	38.0	31.9
ts-Fi8 (177i)	29.9	20.1
ts-EG (396i)	29.8	27.3
ts-Gi9 (189i)	19.6	14.8

Figure S1. Evolution of bond lengths along the IRC for (a) ts-Bi4 (b) ts-Ci7 c) ts-EG (c) ts-Gi9 at M06-2X/6-311++G(d,p) level.

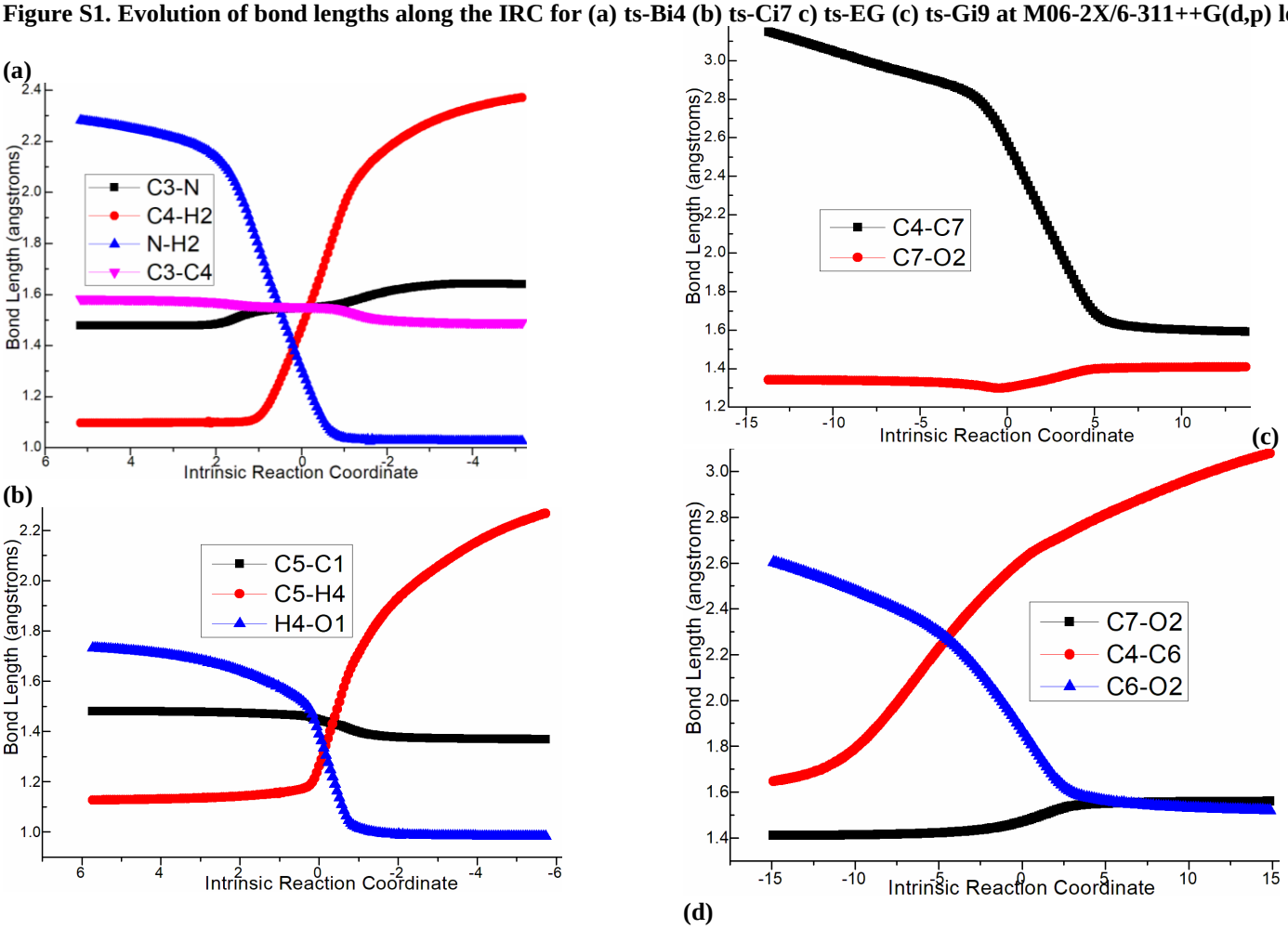

4 Conclusions

The first theoretical investigation was provided by our DFT calculation on Tf_2O-catalyzed [3 + 2 + 1] benzannulation of annular-enaminone with monomeric benzoyl acetonitrile. Activated by Tf_2O, enaminone was initially formed vinyl iminium triflate intermediate, which was captured by benzoyl acetonitrile to initiate selective 1,2-addition and form first TfOH. Next, key trifluorome-thanesulfonate intermediate was generated after elimination of dimethylamine. Subsequently with a second molecule of benzoyl acetonitrile, the reaction took place via Michael-type addition followed by second proton donation. Then competitive 1,4-elimination or 1,2-elimination were possible to complete the release of second TfOH. Finally, the product multisubstituted arylnitrile was obtained through sequential Knoevenagel condensation and aromatization. Michael-type addition was determinated to be rate-limiting from the perspective of whole process. The 1,2-elimination was more favorable within two parallel paths kinetically.

Electronic Supplementary Material

Supplementary data available: [Computation information and cartesian coordinates of stationary points; Calculated relative energies for the ZPE-corrected Gibbs free energies (ΔG_{gas}), and Gibbs free energies (ΔG_{sol}) for all species in solution phase at 353 K.]

Author contributions: Conceptualization, Nan Lu; Methodology, Nan Lu; Software, Nan Lu; Validation, Nan Lu; Formal Analysis, Nan Lu; Investigation, Nan Lu; Resources, Nan Lu; Data Curation, Nan Lu; Writing-Original Draft Preparation, Nan Lu; Writing-Review & Editing, Nan Lu; Visualization, Nan Lu; Supervision, Nan Lu; Project Administration, Nan Lu; Funding Acquisition, Junling Duan. All authors have read and agreed to the published version of the manuscript.

Funding: This work was supported by Key Laboratory of Agricultural Film Application of Ministry of Agriculture and Rural Affairs, P.R. China.

Conflict of interest: The authors declare no conflict of interest

References

1. García-Alvarez, R.; Crochet, P.; Cadierno, V. Metal-catalyzed amide bond forming reactions in an environmentally friendly aqueous medium: Nitrile hydrations and beyond. Green Chem. 2013, 15, 46.
2. Anbarasan, P.; Schareina, T.; Beller, M. Recent developments and perspectives in palladium-catalyzed cyanation of aryl halides: Synthesis of benzonitriles. Chem. Soc. Rev. 2011, 40, 5049.
3. Kim, J.; Kim, H. J.; Chang, S. Synthesis of aromatic nitriles using nonmetallic cyano-group sources. Angew. Chem., Int. Ed. 2012, 51, 11948.
4. Xu, Z.; Liang, X.; Li, H. Oxidative radical transnitrilation of arylboronic acids with trityl isocyanide. Org. Lett. 2022, 24, 9403.
5. Ahmad, M. S.; Zeng, B.; Qasim, R.; Zheng, D.; Zhang, Q.; Jin, Y.; Wang, Q.; Meguellati, K. Ni-catalyzed cyanation of (hetero)aryl halides with acetonitrile as cyano source. ACS Catal. 2024, 14, 2350.
6. Du, T.; Li, S.; He, Y.; Long, H.; Liu, X.; Li, H. B.; Liu, L. Copper-catalyzed [3 + 2 + 1] cycloaddition of alkenes with benzoquinones and dicarbonyl compounds via tandem oxidative dicarbofunctionalization/cyclization sequence. Chin. J. Chem. 2022, 40, 1681.
7. Chen, S.; Zeng, Y.; Zou, W.; Shen, D.; Zheng, Y.; Song, J.; Zhang, S. Divergent synthesis of tetrasubstituted phenols via [3 + 3] cycloaddition reaction of vinyl sulfoxonnium ylides with cyclopropenones. Org. Lett. 2023, 25, 4286.
8. Wei, W.; Cheung, K. K.; Lin, R.; Kong, L. C.; Chan, K. L.; Sung, H. H.; Williams, I. D.; Tong, R.; Lin, Z.; Jia, G. [2 + 2 + 1 + 1] Cycloaddition for de novo synthesis of densely functionalized phenols. Angew. Chem., Int. Ed. 2023, 62, No. e202307251.
9. Singam, M. K. R.; Nagireddy, A.; Maddi, S. R. Base-mediated benzannulation of α-cyanocrotonates with ynones: Facile synthesis of benzonitriles and fluorenes. Green Chem. 2020, 22, 2370.
10. Wang, H.; Li, S.; Wu, X.; Chen, T.; Liu, W.; Liu, X.; Cao, H. Five-component [2 + 2 + 1 + 1] tandem benzannulation leading to multifunctionalized aromatic amines. Org. Lett. 2024, 26, 9648.
11. Wang, Z.; Zhao, B.; Liu, Y.; Wan, J. Recent advances in reactions using enaminone in water or aqueous medium. Adv. Synth. Catal. 2022, 364, 1508.
12. Han, Y.; Zhou, L.; Wang, C.; Feng, S.; Ma, R.; Wan, J. Recent advances in visible light-mediated chemical trans-formations of enaminones. Chin. Chem. Lett. 2024, 35, No. 108977.
13. Zeng, J.; Zhou, T.; Liu, J.; Wan, J. Photocatalytic pyridine synthesis with enaminones and TMEDA under metal-free conditions. J. Org. Chem. 2024, 89, 11060.
14. Fan, S.; Wu, W.; Su, Y.; Han, X.; Wang, Z.; Zhu, J. Co(III)-catalyzed coupling of enaminones with oxadiazolones for imidazole synthesis. Org. Lett. 2024, 26, 7620.
15. Zhang, M.; Liu, M.; Qiu, Y.; Peng, M.; Zhang, Z.; Song, S.; Chen, X.; Yu, F. Silver-catalyzed cascade bis-heteroannulation reaction of enynones and o-hydroxyphenyl enaminones: Access to highly functionalized 3-furylmethyl chromones. Adv. Synth. Catal. 2024, 366, 2363.
16. Duan, X.; Wang, J.; Li, H.; Du, F.; Chen, R.; Lian, W.; Shi, M. Tandem site-selective bromination and highly regioselective Heck reaction of N-allyl enaminones: Chemodivergent synthesis of polysubstituted pyrroles and pyridines. Org. Chem. Front. 2024, 11, 5532.
17. Yang, L.; Wei, L.; Wan, J. Redox neutral [4 + 2] benzannulation of dienals and tertiary enaminones for benzaldehyde synthesis. Chem. Commun. 2018, 54, 7475.
18. Fu, L.; Huang, H.; Jiang, Y.; Liu, X.; Chen, H.; Wan, J. Copper(II)-catalyzed [2 + 2+2] annulation of enaminones with maleimides using a traceless directing group strategy. Adv. Synth. Catal. 2024, 366, 4139.
19. Hu, Y.; Wang, Z.; Xiang, J.; Ma, J.; Lin, R.; Wang, J.; Wu, A. Synthesis of polysubstituted phenols via [3 + 3] condensation reaction from tricarbonyl compounds and readily available enaminones, cinnamaldehydes or arylformyl trifluoroacetones. Tetrahedron 2022, 128, No. 133124.
20. Zhou, S.; Liu, X.; Zhang, T.; Loh, T. P.; Tian, J. Cleavage and

reassembly of 1,3-dicarbonyls with enaminones to synthesize highly functionalized naphthols. Angew. Chem., Int. Ed. 2025, 64, No. e202421374.
21. Huang, H.; Kang, J. Triflic anhydride (Tf 2 O)-activated transformations of amides, sulfoxides and phosphorus oxides via nucleophilic trapping. Synthesis 2022, 54, 1157.
22. Zhang, C.; Guo, H.; Chen, L.; Zhang, J.; Guo, M.; Zhu, X.; Shen, C.; Li, Z. One-pot synthesis of symmetrical and asymmetrical 3-amino diynes via Cu(I)-catalyzed reaction of enaminones with terminal alkynes. Org. Lett. 2021, 23, 8169.
23. Zhang, C.; Lin, J.; Wang, L.; Mei, Y.; Wang, L.; Xie, Y.; Lu, Y.; Tian, J.; Wang, W.; Chen, L.; Guo, M.; Zhou, C. Tf 2 O-mediated tandem reaction of enaminones for the synthesis of functionalized conjugated-enals/β-naphthalaldehydes. J. Org. Chem. 2024, 89, 373.
24. Lin, J.; Tian, J.; Lu, Y.; Xu, Y.; Chen, L.; Jiang, Y.; Guo, M.; Zhang, X.; Zhang, C. Divergent synthesis of enynals and dihydrobenzo[f]isoquinolines via deoxyalkynylation of enaminones enabled by the cooperative action of Tf 2 O/Pd/Cu. J. Org. Chem. 2024, 89, 16419.
25. Zhang, X.; Li, F.; Zhou, Y.; Zhang, J.; Zhou, B.; Chen, L.; Lin, J.; Zhang, C. Synthesis of Multisubstituted Arylnitriles via Tf 2 O-Mediated Benzannulation of Enaminones with Acylacetonitriles. Org. Lett. 2025, 27, 10, 2400–2405.
26. Frisch, M. J.; Trucks, G. W.; Schlegel, H. B. et al. Gaussian 09 (Revision B.01), Gaussian, Inc., Wallingford, CT, 2010.
27. Stephens, P. J.; Devlin, F. J.; Chabalowski, C. F.; Frisch, M. J. Ab initio Calculation of Vibrational Absorption and Circular Dichroism Spectra Using Density Functional Force Fields, J. Phys. Chem. 1994, 98, 11623-11627.
28. Becke, A. D. Density-functional thermochemistry. IV. A new dynamical correlation functional and implications for exact-exchange mixing. J. Chem. Phys. 1996, 104, 1040-1046.
29. Lee, C. T.; Yang,W. T.; Parr, R. G. Development of the Colle-Salvetti correlation-energy formula into a functional of the electron density. Phys. Rev. B 1988, 37, 785-789.
30. Li, X.; Kong, X.; Yang, S.; Meng, M.; Zhan, X.; Zeng, M.; Fang, X. Bifunctional Thiourea-Catalyzed Asymmetric Inverse-Electron-Demand Diels-Alder Reaction of Allyl Ketones and Vinyl 1,2-Diketones via Dienolate Intermediate, Org. Lett. 2019, 21, 1979-1983.
31. Krenske, E. H.; Houk, K. N.; Harmata, M. Computational Analysis of the Stereochemical Outcome in the Imidazolidinone-Catalyzed Enantioselective (4 + 3)-Cycloaddition Reaction, J. Org. Chem. 2015, 80, 744-750.
32. Lv, H.; Han, F.; Wang, N.; Lu, N.; Song, Z.; Zhang, J.; Miao, C. Ionic Liquid Catalyzed C-C Bond Formation for the Synthesis of Polysubstituted Olefins. Eur. J. Org. Chem. 2022, e202201222.
33. Zhuang, H.; Lu, N.; Ji, N.; Han, F.; Miao, C. Bu4NHSO4-Catalyzed Direct N-Allylation of Pyrazole and its Derivatives with Allylic Alcohols in Water: A Metal-free, Recyclable and Sustainable System. Advanced Synthesis & Catalysis 2021, 363, 5461-5472.
34. Lu, N.; Liang, H.; Qian, P.; Lan, X.; Miao, C. Theoretical investigation on the mechanism and enantioselectivity of organocatalytic asymmetric Povarov reactions of anilines and aldehydes. Int. J. Quantum Chem. 2020, 120, e26574.
35. Tapia, O. Solvent effect theories: Quantum and classical formalisms and their applications in chemistry and biochemistry. J. Math. Chem. 1992, 10, 139-181.
36. Tomasi, J.; Persico, M.; Molecular Interactions in Solution: An Overview of Methods Based on Continuous Distributions of the Solvent. Chem. Rev. 1994, 94, 2027-2094.
37. Simkin, B. Y.; Sheikhet, I. Quantum Chemical and Statistical Theory of Solutions—A Computational Approach, Ellis Horwood, London 1995.
38. Tomasi, J.; Mennucci, B.; Cammi, R. Quantum Mechanical Continuum Solvation Models. Chem. Rev. 2005, 105, 2999-3093.
39. Marenich, A. V.; Cramer, C. J.; Truhlar, D. G. Universal Solvation Model Based on Solute Electron Density and on a Continuum Model of the Solvent Defined by the Bulk Dielectric Constant and Atomic Surface Tensions. J. Phys. Chem. B 2009, 113, 6378–6396.
40. Reed, A. E.; Weinstock, R. B.; Weinhold, F. Natural population analysis. J. Chem. Phys. 1985, 83, 735-746.
41. Reed, A. E.; Curtiss, L. A.; Weinhold, F. Intermolecular interactions from a natural bond orbital donor-acceptor view point. Chem. Rev. 1988, 88, 899-926.
42. Foresman, J. B.; Frisch, A. Exploring Chemistry with Electronic Structure Methods, 2nd ed., Gaussian, Inc., Pittsburgh 1996.
43. Lu, T.; Chen, F. Multiwfn: A multifunctional wavefunction analyzer. J. Comput. Chem. 2012, 33, 580-592.